XMM-Newton X-ray spectra of Mrk 273 and Mrk 273x

02.10.2021

This research has made in the Center for the Collective Use of Scientific Equipment "Laboratory of high energy physics and astrophysics"

1 General properties

Mrk 273 is one of the nearest Ultra-Luminous Infrared Galaxy (ULIRG) – 176 Mpc, $z = 0.03734 \pm 0.00001$), and is a good laboratory to investigate the effects of dual AGN activity. Mrk 273 is a late merger with dual nuclei in the midinfrared, **located 0.75 kpc apart in projection (at an angular distance for the observer about 1")** [1]. It's morphological type is peculiar galaxy, nuclear activity classified as Seyfert 2, alternative classification in NED [1], is Low Ionization Nuclear Emission Line Region type 2 (LINER 2). In active galactic nuclei of type 2, the central region is obscured by structures of a gas-dust torus and a galaxy.

Mrk 273 in the Sloan Digital Sky Survey [2] (SDSS-IV DR16) [2] has ID SDSS J134442.16+555313.5. It was automatically classified by the SDSS spectrograph as "galaxy AGN broadline". SDSS spectrograph does not distinguish two separate nuclei of the galaxy. The nuclear spectrum is typical for Seyfert 2 with narrow forbidden identified lines of oxygen, nitrogen, sulfur, argon – [OII] 3725+3727, [OIII] 4959+5007, [OI] 6300+6360, [NII]

[1] https://ned.ipac.caltech.edu
[2] https://www.sdss.org/dr16

6548+6583, [SII] 6716+6730, [ArIII] 7135 and emission hydrogen (Hα, Hβ, Hγ, Hδ).

Vivian U, et al. presented near-infrared integral-field spectra and images of the nuclear region of Mrk 273 taken with OSIRIS (OH-Suppressing Infra-Red Imaging Spectrograph) and NIRC2 (The second generation Near Infrared Camera) on the Keck II Telescope with laser guide star adaptive optics. They confirmed the presence of the hard X-ray AGN in the southwest nucleus. In the north nucleus, they found a strongly rotating gas disk whose kinematics indicate a central black hole of mass $(1.04 \pm 0.1) \cdot 10^9 M_\odot$ [3].

NuSTAR (Nuclear Spectroscopic Telescope Array) observed Mrk 273 during guaranteed time on 2013 November 14. The authors proceed to model the NuSTAR spectrum with two absorbed nuclei, SW and NE. The NE nucleus is hypothesized to have an X-ray source absorbed by a larger nH than that for SW and they assumed that each nucleus has an X-ray source with the standard power-law slope of $\Gamma = 1.9$ [4].

Mrk 273 was detected at X-ray energies by Chandra [5]. The active galactic nuclei (AGNs) was confirmed by Chandra's data. First AGN was associated with the Southwest nucleus and a second hard X-ray (4-8 keV) point source was detected and coincident with the Northeast nucleus at a projected distance of 0.75 kpc from the Southwest (SW) nucleus. The hard X-ray spectrum of the Northeast (NE) nucleus is consistent with a heavily absorbed AGN [1].

We also descry Mrk 273x, a background weak source in the Mrk 273 field about $1.3'$ away. This AGN has an X-ray luminosity of $L_X = 2.43 \cdot 10^{44}\ erg\ s^{-1}$ in the 0.5-10 keV band at $z = 0.458$ [5]. It's classification in NED is unobscured Seyfert 2. Mrk 273x optical properties are similar to Seyfert 2 but its X-ray properties resemble those of Seyfert 1 galaxies [5].

2 XMM observations and spectral fitting

XMM Newton (The X-ray Multi-Mirror Mission) is used to study different types of AGN, their physical processes and structures, detect variability. We used data from PN camera because pn-type CCDs (Charge-Coupled Devices) are mounted in the focal plane therefore the photon beam is directed onto the camera without interruptions. The PN camera has an entire field of view 30 arcmin, effective detector area 1227 cm^2, angular resolution – the full width at half maximum (FWHM) of the point spread function (PSF) is 6.6 arcsec,

energy range from 0.2 to 15 keV [6], but effectively works only in the range up to 10 keV. An energy resolution is $E/dE = 20 - 50$. The data extraction was performed with the Science Analysis System (SAS) [7] version 16.0.0.

Mrk 273 was observed by XMM Newton [3], 2 times – during 22840 s in 2002-05-07 (ID 0101640401) and 22800 s in 2013-11-04 (ID 0722610201). The observation ID 0722610201 is better than ID 0101640401. Their filtered images can be seen in Pic.1, Pic.3. XMM-Newton is not able to view two nuclei of Mrk 273, its angular resolution is only 7", so we see the summaried radiation of two nuclei. But, as already mentioned above, the NE nucleus is obscured so its X-ray spectrum is described by an absorbed, Compton-thick simple power-law.

In our opinion, the main contribution to the total spectrum and it's details gives the SW nucleus.

A typical X-ray spectrum of AGN is composed from the following components [8]: an underlying power-law continuum due to thermally Comptonized soft photons with absorption due to the obscuring torus (*powerlaw*phabs* model); a soft excess at low energies below 1 keV due to thermal emission from an optically-thick accretion disk (*bmc* model); a fluorescent/recombination FeKα line (*zgauss* model); a Compton hump due to X-ray reflection from the disk (*bmc* model).

Let's analyze obs. ID 0722610201 first. Mrk 273 spectrum demonstrate all of AGN components. Its spectrum was fitted with complex model

*powerlaw*phabs+bmc+apec+zgauss* (see Pic. 2, Table 1).

The low-energy spectrum of (U)LIRGs is dominated by a combination of a thermal plasma component with temperature $kT \gtrsim 0.7\ keV$, particularly important at $E < 3keV$, and the emission from high-mass X-ray binaries (HMXBs) at $1 < E(keV) < 10$ [9], [10]. For the HMXB population, we assumed a power-law given by $\Gamma = 1.5$. For the thermal component, in some cases it is able to account the soft excess by single temperature *black-body* model. However, the source shows additional components in the 0.2 – 10 keV energy band, such as a spectral hardening at $E > 5keV$ (the so-called Compton Hump), as well as absorption and emission features [11]. In our case, soft excess and a Compton Hump are taken into account by *bmc* (Comptonization by relativistic matter) model. This is an analytic model describing Comptonization of soft photons by matter undergoing relativistic bulk-motion [7]. The model parameters are the characteristic black-body

[3]http://xmm-catalog.irap.omp

temperature of the soft photon source T_S, a spectral (energy) index α, and an illumination parameter characterizing the fractional illumination of the bulk-motion flow by the thermal photon source [12]. α connects with power-law index $\Gamma = 1 + \alpha$. As it was seen from a work S. Giacchè, R. Gilli, L. Titarchuk [11] and a work of Gliozzi et al. [13] black-body spectral fit of the soft excess for AGNs hosting BHs whose mass is $\sim 10^7 - 10^9 M_\odot$ the expected value spans the range $kT_{exp} \sim 10 - 40\ eV$, whereas the usual fit value is $kT_{fit} \sim 0.1\ keV$. We selected the value that gave the best fit to the spectrum with other previously known parameters. The feature around $\sim 0.7\ keV$ we tried to account by adding an *apec* component. The nature of this absorption edge in the range $\sim 0.7 - 0.74\ keV$ has been widely debated. Most likely, this feature of the spectrum in Mrk 273 is identified with an absorption K-edge of OVII since it manifests itself same quite often in other objects [11], [14]. The narrow emission FeKα line has been observed at $\sim 6.4\ keV$, it suggests an origin from cold (FeI-XV) matter distant from the inner disk region. It was fitted by *zgauss* model.

We also should included in this modelling the absorption associated to the interstellar medium in our own Galaxy with the second *phabs* component and it should affects the whole model (multiplying by the sum of all fitting terms). The value of the Galactic column density in the direction of Mrk 273 and Mrk 273x has been fixed to $nH = 7.3 \cdot 10^{19}\ cm^{-2}$, showing weak absorption (the value was obtained using a calculator at https://heasarc.gsfc.nasa.gov/cgi-bin/Tools/).

Contrary to other's authors previous work [5], we decided to fit the Mrk 273x spectrum with typical parameters for Seyfert 2. Mrk 273x spectrum was fitted with combined model *powerlaw*phabs+bmc* (see Pic. 2, Table 1). Its X-ray spectrum is described by an absorbed power-law with $\Gamma = 1.9$, $nH = 3{\cdot}10^{23} cm^{-2}$. There is no cutoff at low energies so we take it into account with added the *bmc* model. The FeKα line is not detected. Therefore, Mrk 273x exhibits unusual properties and therefore requires unusual approaches, which, of course, requires further research.

Now consider obs. ID 0101640401 in detail (see Pic. 3, Table 1). Unfortunately, the Mrk 273x is located on the chip separation line and the image of Mrk 273 is worse than the previous observation. We fitted Mrk 273 spectrum obs. ID 0101640401 with the same parameters as in obs. ID 0722610201, which didn't reflect any changes in the nucleus activity.

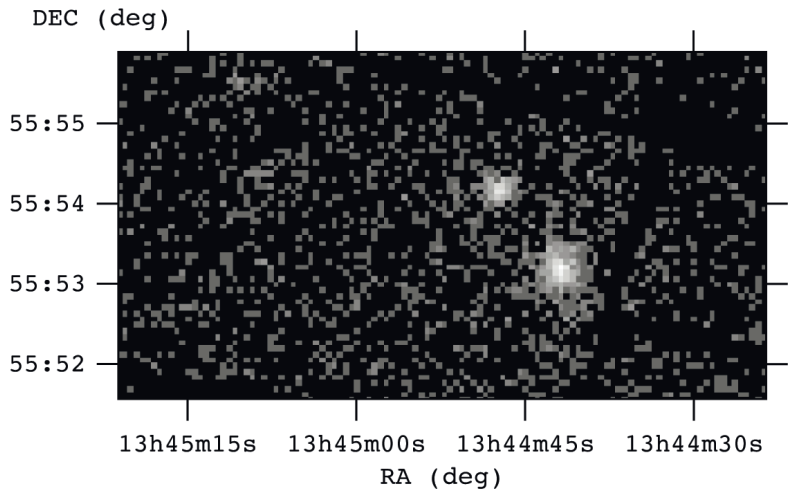

Рис. 1: Image of Mrk 273 (lower brighter image with a visible decrease in brightness from the center to the edges) and Mrk 273x (upper image) in the 0.1-10 keV band (obs. ID 0722610201). The image is shown in gray scale and in units of counts.

3 The soft excess and reflections about emission state of AGN

The definition of soft excess corresponds to the increase in flux measured above the underlying power-law continuum at $E < 1keV$ [11]. The nature of this peculiarity can be described by the thermal emission from the innermost layers of the accretion disc that emit a modified black-body spectrum [15]. We assume that most of the inner accretion disc luminosity is a perfect black-body emission coming from within a distance $r = 3R_g$ from the centre, $R_g = GM/c^2$ is the gravitational radius, G – gravitational constant, c – light speed. From the Stefan-Boltzmann law we get $L \cong 4\pi r\sigma_B T^4$, where $\sigma_B = 5.67 \cdot 10^{-5}\ erg\ cm^{-2}\ s^{-1}\ K^{-4}$ is the Stefan-Boltzmann constant and $2\pi r^2$ is the surface of the two-sided disc. We provide that the luminosity equals some fraction λ of the Eddington luminosity $L_E = 1.26 \cdot 10^{38} M_{BH}/M_\odot\ erg\ s^{-1}$. Where $\lambda = \dot{m}$, $\dot{m}$ – total Eddington-scaled mass accretion rate, it depends of the accretion flow in different spectral states.

Black holes manifest themselves in rather distinct spectral (may be tem-

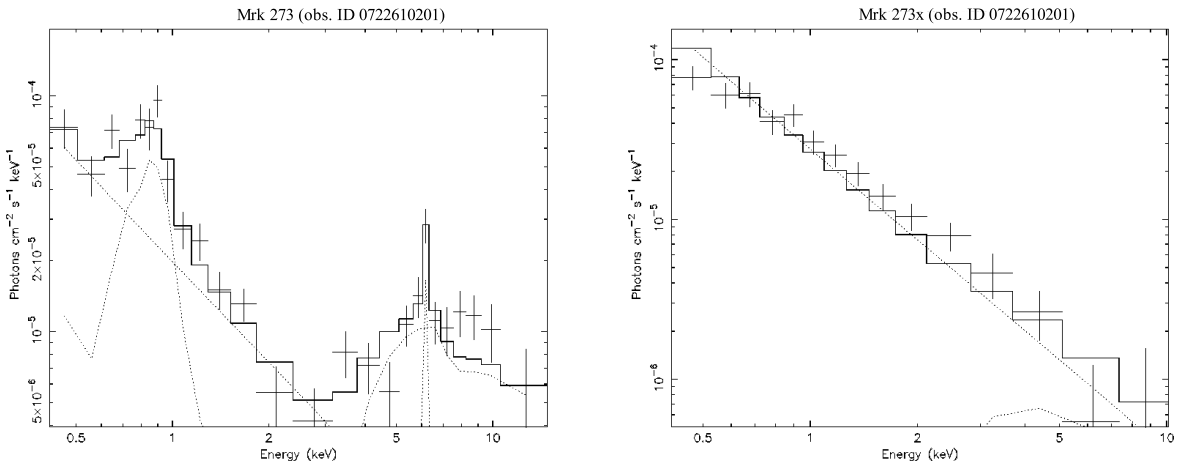

Рис. 2: The XMM-Newton EPIC PN spectrum of Mrk 273 and Mrk 273x in the 0.1-10 keV band plotting with the best-fit models (obs. ID 0722610201). The best-fit parameters are summarized in Table 1. The model is shown in solid lines and the components of it are shown in dotted lines.

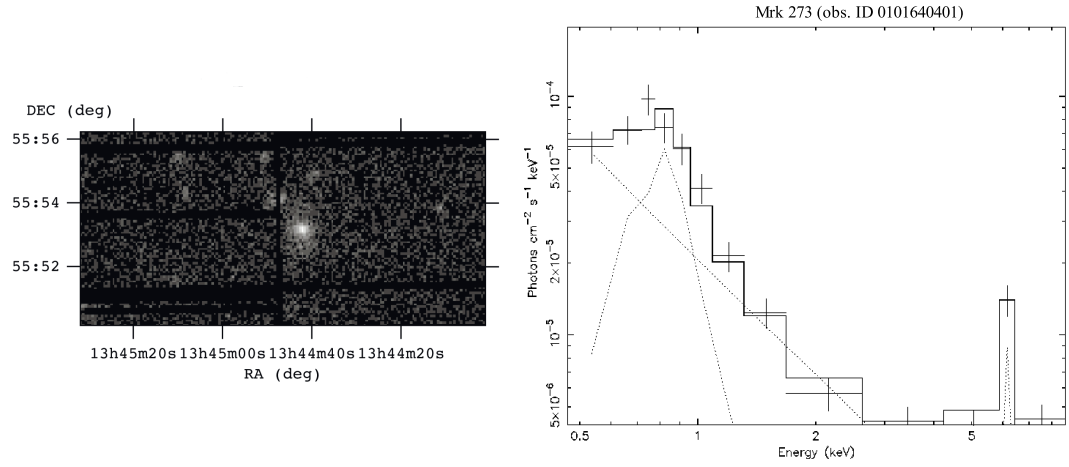

Рис. 3: The XMM-Newton EPIC PN observation (*left* pannel) and spectrum (*right* pannel) of Mrk 273 in the 0.1-10 keV band (obs. ID 0101640401) plotting with the best-fit models. The fit parameters are summarized in Table 1.

poral) states defined in the 1-10 keV band [16],[17],[18]. Below, we dwell

in more detail in the hard emission state. This is the case implemented at low luminosities, when the jet-corona coupling dominates the energy output [16], [18]. The hard state mostly includes low-luminosity AGN ($\lesssim 10^{-3} L_E$) characterized by low-excitation radio-loud nuclei and a negligible disc contribution and could be identified with the bright hard and intermediate states (half of Seyfert 2 nuclei and the bright LINERs) [16]. Their hosts show ongoing star formation in the central kiloparsecs. There is the difficulty to measure the disc contribution in intermediate-to-low luminosity AGN, i.e. below $\lesssim 10^{43}\ erg\ s^{-1}$, since this is heavily absorbed due to the large hydrogen opacity in the Lyman continuum (in addition to contamination from the stellar population in the host galaxy). Low excitation sources are typically dominated by the power-law continuum (synchrotron/inverse-Compton), with some or negligible contribution from a cold accretion disc (UV-emitting).

If we assume, with some restrictions (see for example [17]), the existence of similar states of activity identified in supermassive and stellar mass black holes, then we should accept the following for the hard state.

The hard state is well characterized by such conditions – the spectrum is dominated ($> 80\%$ at 2-20 keV) by a power-law, the spectral index is in the range $1.5 \lesssim \Gamma \lesssim 2.1$. In this state, the disk is either not detected at 2-10 keV it appears much cooler (and larger?) than it does in the soft state [16]. In the soft state the power-law component is observed to be steeper ($\Gamma \sim 2.5$).

A standard accretion disc of BH with masses $10^6 - 10^9 M_\odot$ accreting at $\sim 0.001 - 1.1 L_E$ [13]. At low luminosity ($10^{-4} L_E \lesssim L_X \lesssim 10^{-2} L_E$) the spectrum is hard. And it is a question if this hard state could extend up to a several times $10^{-1} L_E$.

E. Seifina, A. Chekhtman, L. Titarchuk show that BH mass correlate with spectral index and accretion flow [19]. They estimated analytically that the *bmc* spectral index α rises from ~ 0.7 in hard state. The emergent spectrum becomes softer when the illumination of the inner accretion flow by the soft (disk) photons increases.

The goal of this work was to obtain an X-ray spectrum for Mrk 273 and Mrk 273x from XMM-Newton observations, which was achieved. The disadvantage is a rough estimate of the temperature of the inner accretion disk. The relationship between the spectral index and the coefficient λ should be better investigated to establish the state of accretion.

Табл. 1: Spectral fitting results with the Xspec models for Mrk 273 and Mrk 273x.

Object	nH, $10^{22} cm^{-2}$	Pho Index, Γ	kT_S, keV	α	kT, (apec) keV	Line FeKα keV	$\chi^2/d.o.f.$
Mrk 273 ID 0722610201	30	1.5	0.01	0.43± 0.17	0.88± 0.06	6.4	29.43/26
Mrk 273 ID 0101640401	30	1.5	0.01	0.64± 0.17	0.77± 0.07	6.4	10.48/13
Mrk 273x ID 0722610201	10	1.9	0.01	0.9	-	-	26.79/15

4 Acknowledgment

This research has made use of data obtained from the 4XMM XMM-Newton serendipitous source catalogue compiled by the 10 institutes of the XMM-Newton Survey Science Centre selected by ESA.

We acknowledge the usage of the HyperLeda database.

This research has made use of the NASA/IPAC Extragalactic Database (NED), which is operated by the Jet Propulsion Laboratory, California Institute of Technology, under contract with the National Aeronautics and Space Administration.

References

[1] W. Liu, S. Veilleux, K. Iwasawa, et al. The Astrophys. J., **872**, 39 (2019); https://doi.org/10.3847/1538-4357/aafdfc.

[2] R. Ahumada, et al. The Astrophys. J. Suppl. Series **249**, 1 (2020); https://doi.org/10.3847/1538-4365/ab929e.

[3] V. U, A. Medling, D. Sanders, et al. The Astrophys. J. **775**, 115 (2013); https://doi.org/10.1088/0004-637X/775/2/115.

[4] K. Iwasawa, V. U, J. M. Mazzarella, et al. Astron. Astrophys. **611**, A71 (2018); https://doi.org/10.1051/0004-6361/201731662.

[5] X. -Y. Xia, S. J. Xue, S. Mao, et al. The Astrophys. J. **564**, 196 (2002); https://doi.org/10.1086/324187.

[6] D. H. Lumb, R. S. Warwick, M. Page, A. De Luca Astron. Astrophys. **389**, 93 (2002); https://doi.org/10.1051/0004-6361:20020531.

[7] Users Guide to the XMM-Newton Science Analysis System Issue 16.0 15.03.2021. URI: https://xmm-tools.cosmos.esa.int/external/xmm_user_support/documentation /sas_usg/USG/

[8] A. C. Fabian Astronomische Nachrichten, **327**, 943 (2006); https://doi.org/10.1002/asna.200610669.

[9] E. Treister, C. M. Urry, K. Schawinski The Astrophys. J. Lett. **722**, L238 (2010); https://doi.org/10.1088/2041-8205/722/2/L238.

[10] M. Persic, Y. Rephaeli Astron. Astrophys. **382**, 843 (2002); https://doi.org/10.1051/0004-6361:20011679.

[11] S. Giacchè, R. Gilli, L. Titarchuk Astron. Astrophys. **562**, A44 (2014); https://doi.org/10.1051/0004-6361/201321904.

[12] K. Arnaud, C. Gordon, B. Dorman Xpec An X-Ray Spectral Fitting Package 12.11.1 31.03.2020; https://heasarc.gsfc.nasa.gov/xanadu/xspec/manual/manual.html.

[13] M. Gliozzi, L. Titarchuk, S. Satyapa, et al. The Astrophys. J., **735**, 16 (2011); https://doi.org/10.1088/0004-637X/735/1/16.

[14] K. M. Leighly, R. F. Mushotzky, T. Yaqoob, The Astrophys. J. **469**, 147 (1996); https://doi.org/10.1086/177767.

[15] C. Done, S. W. Davis, C. Jin, et al. MNRAS, **420**, 1848 (2012); https://doi.org/10.1111/j.1365-2966.2011.19779.x.

[16] J. A. Fernández-Ontiveros, T. Muñoz-Darias MNRAS, **504**, 5726 (2021); https://doi.org/10.1093/mnras/stab1108.

[17] E. G. Körding, S. Jester, R. Fender MNRAS, **372**, 1366, (2006); https://doi.org/10.1111/j.1365-2966.2006.10954.x.

[18] F. Panessa, R. D. Baldi, A. Laor, et al. Nat. Astron. **3**, 387 (2019); https://doi.org/10.1038/s41550-019-0765-4.

[19] E. Seifina, A. Chekhtman, L. Titarchuk Astron. Astrophys. **613**, A48 (2018); https://doi.org/10.1051/0004-6361/201732235.

[20] J. E. McClintock, R. A. Remillard Black hole binaries Chapter 4 in "Compact Stellar X-ray Sources,"eds. W.H.G. Lewin and M. van der Klis, Cambridge University Press (2004); https://doi.org/10.2277/0521826594.